

## Electrodeposition of Pt–Ru Alloy Electrocatalysts for Direct Methanol Fuel Cell

Chao Li<sup>1</sup>, Ruihui Dai<sup>2</sup>, Ruifang Qi<sup>2</sup>, Xiaojia Wu<sup>3</sup> and Jingjun Ma<sup>3,\*</sup>

<sup>1</sup> College of Sciences, Agricultural University of Hebei, Baoding 071001, P.R. China

<sup>2</sup> Department of Basic Courses, Agricultural University of Hebei, Huanghua 061100, P.R. China

<sup>3</sup> College of Science and Technology, Agricultural University of Hebei, Huanghua 061100, P.R. China

\*E-mail: [jingjunma\\_hebeiag@foxmail.com](mailto:jingjunma_hebeiag@foxmail.com)

Received: 26 November 2016 / Accepted: 5 January 2017 / Published: 12 February 2017

---

The electrocatalyst based on Pt-Ru alloy was successfully prepared on the carbon paper through electrodeposition approach. The deposition potential and time was tuned to control the particle size and density. Brunauer-Emmett-Teller (BET) isotherms, scanning electron microscopy (SEM), X-ray diffraction (XRD) and X-ray photoelectron spectroscopy were used to characterize the catalyst particles. The highest catalytic activity was observed with the Pt-Ru electrocatalyst towards the oxidation of methanol, Besides, the Pt-Ru electrocatalyst also exhibited the most tolerance against the poisoning of CO.

---

**Keywords:** Electrocatalyst; Pt-Ru alloy; Electrodeposition; Methanol fuel cell; Carbon monoxide poisoning

### 1. INTRODUCTION

Along with the fast growth in population as well as economic and social development, the demand of energy has been continuously increasing in an age. Fossil fuels have been primary energy source for human beings since the dawn of the industrial revolution begins. Approximate 64% of the total electricity is produced with crude oil, coal and natural gas, whereas the rest is provided with renewable energy sources including the wind, solar and hydro energy [1, 2]. The global oil reserves are sufficient for the further 40 years based on the current level of oil production and consumption. Nevertheless, the current oil reserves are supposed to be consumed at much faster rate because of the exploding economic growth and population in numerous parts of the world such as China and India. In the case of coal reserves, they are assumed to adequate for more than 150 years. A relatively new

methane reserves in the form of hydrates have been discovered compared to oil and coal, which are estimated to be 20 folds of the total reserves of gas, oil and coal. Besides, the technique, which is required for the extraction of those methane hydrates in the ocean, is predicted to be ready in 10 years [3].

Since the 1960s, the methanol electro-oxidation has been an intensive interest, because of the promising properties of methanol acting as fuel. A rate determining step mode, which contains a series of the dehydrogenation procedures followed by the reactions between the absorbed intermediates and the surface hydroxyl radicals, have been employed to clarify the reaction mechanism. More than one pathways have been involved in the mechanism of the electro-oxidation, whereas some of them do not induce the generation of CO<sub>2</sub>. As matter of fact, it is demonstrated that CO<sub>2</sub> is not the primary product of the oxidation, where the other electro-oxidation products contain formaldehyde (CH<sub>2</sub>O) and formic acid (HCOOH).

Numerous bimetallic catalysts based on Pt have been reported during the past two decades [4-6]. Owing to the remarkable catalytic activity towards oxidizing methanol and the strong tolerance against the poisoning of carbon monoxide [7-9], Pt-Ru alloy-based catalyst has been a primary candidate as the DMFCs anode among them. The intermediate CO could be easily oxidized with Ru in the Pt-Ru alloy through the bifunctional mechanism [10-13]. However, the capacity of the alloy catalyst of Pt-Ru towards the oxidation of methanol still requires to be enhanced [14, 15]. Thus, three primary issues require to be taken in account, including the nature of the support, the morphology of the nanoparticles and the addition of the third metal [16, 17], so that to reduce the cost and improve the catalytic activity of the Pt-Ru alloy.

So far, numerous approaches, including impregnation [18], microemulsion [19], colloidal [20], electrodeposition [21] and sputtering [22], have been reported to produce the Pt-Ru alloy catalyst. Because of the capacity to control the composition, density and size of the catalyst, electrodeposition exhibits superior compared with other approaches. Besides, the improve catalyst utilization as well as a simple preparation approach could also be provided through electrodeposition [23]. Moreover, compared with the chemical reduction approach, a high purity of the deposits could be guaranteed with this method, where the impurities generated from the electrolyte could be easily introduced into the catalysts through the chemical reduction process [24]. Diverse substrates including the carbon nanotube, highly ordered pyrolytic graphite [25] and diamond [26] have been used to study the co-electrodeposition of Pt-Ru catalysts in one step. Owing to the difficulty of generating the triple-phase boundary, these methods exhibit a restriction of the direct application, although the catalysts displayed high capacity based on the electrochemical measurement. However, due to the structural property induced the formation of the triple phase boundary, a carbon paper, which is generally employed in fuel cell as a gas diffusion layer, is available for the co-electrodeposition of Pt-Ru catalyst in one step. The co-electrodeposition of the Pt-Ru electrocatalysts on the carbon paper has already been reported by Jow et al. [21] with massive repeated cycles of double-potential pulse approach. The low-uniformity catalyst particles with a size of around 500 nm covered most part of the carbon paper after 2000 cycles of the repeated dual potential pulses.

Herein, an electrodeposition method was employed to deposit an electrocatalyst based on Pt-Ru onto the carbon paper in one step. ICP-MS, SEM, XPS and XRD were employed to analyse the

structural features of the catalysts. Thereafter, the electrochemical processes were used to study the catalytic performance towards the oxidation of methanol and the tolerance against the poisoning of carbon monoxide.

## 2. EXPERIMENTS

### 2.1. Chemicals

$\text{H}_2\text{PtCl}_6 \cdot 6\text{H}_2\text{O}$  and  $\text{RuCl}_3 \cdot 3\text{H}_2\text{O}$  were commercially available (Capot Chemical Co., Ltd., China). An EASY pure compact ultrapure water system (Barnstead Co., USA) was employed to purify the deionized water ( $\rho = 18.3 \text{ M cm}$ ) with a pH of 7 at  $20 \pm 1 \text{ }^\circ\text{C}$ . NaOH (99%) was purchased from Merck. Carbon paper was bought in Cabot Corporation.

### 2.2. Pt-Ru electrodeposition

A potentiostat (263A, EG&G) was used to control all the electrochemical processes, where a standard three-electrode cell system was employed. A saturated calomel electrode (SCW, Sigma Aldrich) and a Pt wire were utilized as the reference and counter electrodes, respectively. Pt-Ru was electrodeposited at room temperature under atmospheric pressure, where different solutions containing  $\text{RuCl}_3 \cdot x\text{H}_2\text{O}$  and  $\text{H}_2\text{PtCl}_6 \cdot 6\text{H}_2\text{O}$  in 300 mL deionized water was used. HCl or KOH was used to control the pH of the solution at 2.0. Besides, the ratio of the two metal was changed when fixing the total concentration at 20 mM.  $\text{Pt}_2\text{Ru}_{18}$ ,  $\text{Pt}_5\text{Ru}_{15}$ ,  $\text{Pt}_{10}\text{Ru}_{10}$ ,  $\text{Pt}_{15}\text{Ru}_5$  were prepared in this work.

### 2.3. Characterizations

Scanning electron microscopy (SEM) was used to study the microstructure of the sample. Besides, SEM combined with the energy dispersive x-ray spectroscopy (EDAX) was also employed to analyze the quantity and distribution of the elements. X-ray diffraction (XRD) was employed to carry out the qualitative phase analysis of the electro-catalyst with the Philips XPERT PRO system, where Cu  $\text{K}\alpha$  radiation ( $\lambda = 0.15406 \text{ nm}$ ) was used with an operating current and voltage of around 40 mA and about 45 kV, respectively. An ESCALab220i-XL electron spectrometer purchased from VG scientific was used to measure the X-ray photoelectron spectroscopy (XPS) data with Al  $\text{K}\alpha$  radiation of 300 W, where the base pressure was approximate  $3 \times 10^{-9} \text{ mbar}$ . The adventitious carbon with a C1s line at 284.8 eV was used as the reference for the binding energies. Nitrogen adsorption-desorption studies were conducted on the Brunauer-Emmett-Teller (BET) isotherms to determine the specific surface area (SSA).

#### 2.4. CO stripping

The adsorption of carbon monoxide was performed at the working electrode in  $\text{HClO}_4$  solution (0.5 M) saturated with CO for 120 s, where the adsorption potential was 50 mV. Ar was bubbled into the solution to remove the excess CO for 30 min, where the potential of the electrode was maintained at the adsorption potential. Then, the potential was changed to 0.1 V from 0.02 V after the dissolved CO was removed, where a scan rate was 10 mV/s.

#### 2.5. Methanol oxidation reaction

The oxidation experiments of methanol were performed in a solution involving  $\text{H}_2\text{SO}_4$  (0.5 M) and methanol (2.0 M) at room temperature, where chronoamperometry and cyclic voltammetry approaches were employed. The cyclic voltammograms were collected from 0.02 to 1.0 V at 10 mV/s, whereas the onset potential was collected in  $\text{H}_2\text{SO}_4$  solution with a concentration of 0.5 M through the anodic scan. Moreover, the chronoamperometry measurements were also conducted with a constant potential of 0.5 V in the same solution for 3000 s.

### 3. RESULTS AND DISCUSSION

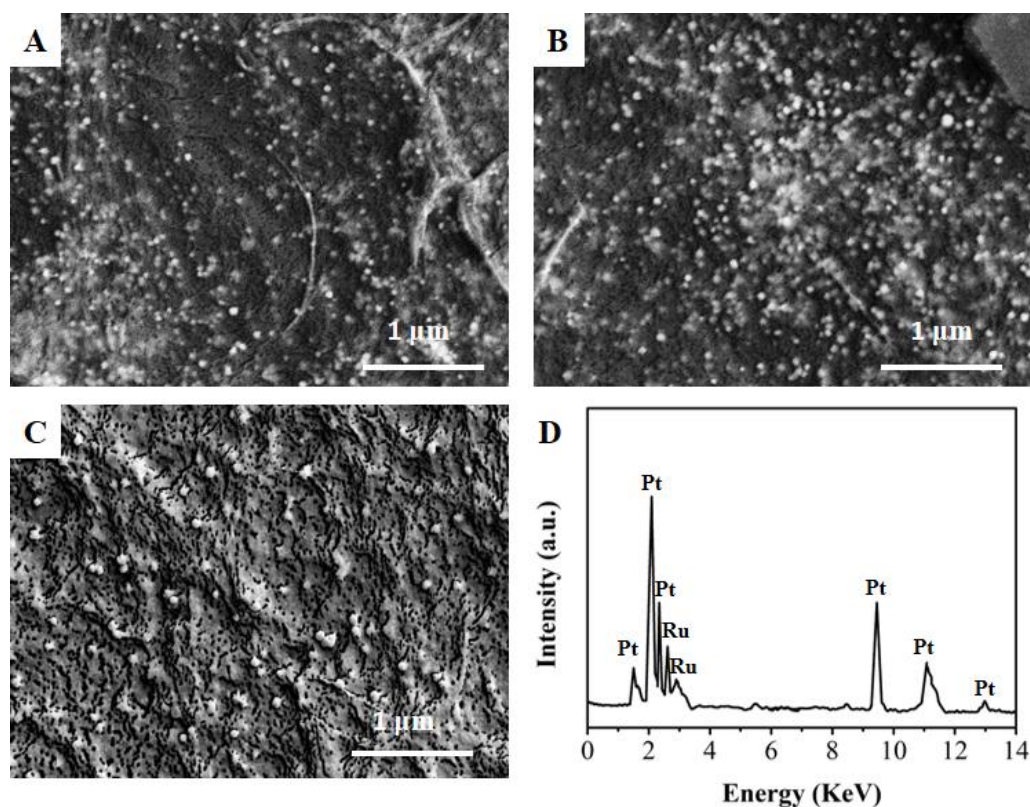


**Figure 1.** The SEM images of the Pt-Ru particles deposited on the carbon paper in the presence of Pt-Ru electrolyte under diverse deposition time and potentials: (A) -0.76 V for 2 s; (B) -0.96 V for 2 s; (C) -1.16 V for 2s. (D) EDX spectrum of the Pt-Ru.

The FESEM images of the Pt-Ru particles was illustrated in Figure 1, which were obtained through changing the deposition time and potential with Pt-Ru electrolyte. An increase of the particle density as well as a decrease of the particle size was observed when more negative potential was applied to the carbon paper with the same deposition time. However, the particle size was also increased with the deposition time, where Pt-Ru particles was deposited on the most part of the carbon paper at -1/16 V for 5 s. Based on the results of particle size and density, it seems that the coverage of Pt-Ru catalyst particles was proportional to the Ru concentration of the electrolytes. Furthermore, without Ru, the particle density (Fig. 2i) was remarkably lower than that obtained with low electrolyte. The energy X-ray spectroscopy (EDX) of the catalyst based on Pt-Ru was clarified in Figure 1D. The results indicated that the major composition was Pt and Ru, which confirmed the Pt-Ru nanoparticles was deposited on the carbon paper.

The XRD patterns of the bare carbon papers as well as the Pt-Ru deposited carbon papers were explicated in Figure 2. The Pt (111) peaks shifted significantly towards higher angle from 39.8 to 40.2° when increasing the mass ratio of Ru. These results suggested that the particles exhibited an alloy structure with single fcc crystal structure [27, 28]. According to the XRD patterns, the peak intensity decreased and the peak broadened when the Pt ratio in the catalyst decreased, which were ascribed to the small amount of Pt-Ru alloy present in the deposits. The decrease in (111) peak intensity as well as an increase in peak broadening with a decrease in Pt are shown in the XRD patterns as the Pt ratio decreased in the catalyst.

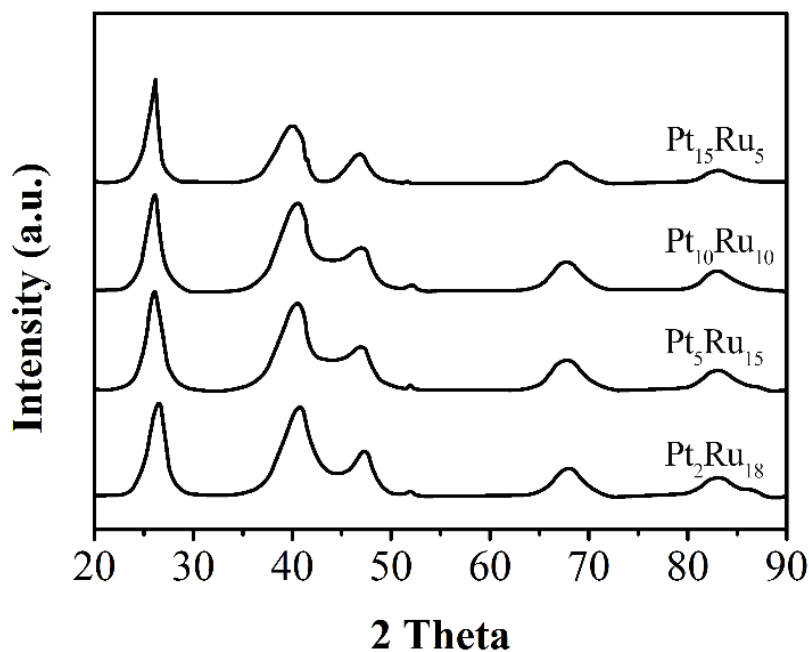


**Figure 2.** XRD patterns of the bare and Pt-Ru in various ratios deposited on the carbon paper.

XPS was employed to analyze the chemical nature of the as-obtained Pt-Ru alloy. Figure 3A and 3B illustrated the spectra of Pt 4f and Ru 3p of Pt-Ru, respectively. However, the absence of the

peak at 73.7 and 74.5 eV corresponded to  $\text{Pt}^{2+}$  and  $\text{Pt}^{4+}$ , respectively, indicated that Pt in the nanoparticles was in zero-valent metallic state. Besides, compared to the pure Pt, of which Pt  $4f_{7/2}$  and Pt  $4f_{5/2}$  located at 71.17 and 74.51 eV, respectively, the 4f XPS spectrum of Pt in the Pt-Ru shifted -0.07 and -0.19 eV, respectively, suggesting that the electronic structure of Pt changed when alloying with Ru. Besides, instead of the Ru  $3d_{3/2}$  at 280 eV, the Ru  $3p_{3/2}$  was utilized to analyze the surface, as the Ru $3d_{3/2}$  overlapped with C1s peak. Taking in account of the contribution of Ru at 460.22 eV as well as  $\text{RuO}_2$  at 461.13 eV, the  $3p_{3/2}$  peak of Ru was deconvoluted. The oxygen atom from functional groups such as quinoid, carbonyl and carboxyl, which were generated during electrochemical pre-treatment, serves as one of the two axial ligands when the planar complex of Pt(II) is oxidized to form the octahedral complex of Pt(IV) [29].

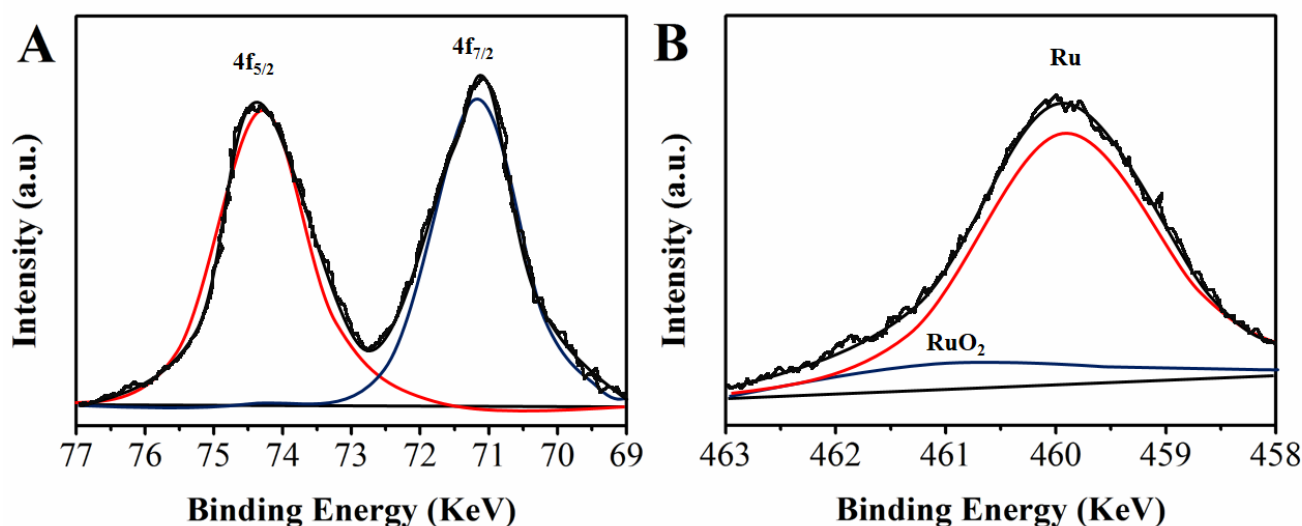


**Figure 3.** X-ray photoelectron spectra of (A) Pt 4f and (B) Ru 3p of the Pt-Ru.

The BET technique was employed to measure the specific surface area of Pt-Ru, which was calculated to be  $99.4 \text{ m}^2/\text{g}$ . Nevertheless, the electrochemical active surface area (ECSA), which was effective for the electro-oxidation of methanol, determined the electrochemical capacity of the electrocatalyst composed of Pt-Ru. The understanding of the number of the electro-active sites, which were available on the surface of the catalyst when the reaction occurred, could be provided by the measured ECSA and is crucial towards the electrochemical capacity of the catalyst. Hence, the CO stripping voltammetry was conducted in  $\text{H}_2\text{SO}_4$  (0.5 M) at  $25^\circ\text{C}$  to determine the ECSA of Pt-Ru, where CO was absorbed on the surface of catalyst at around 0 V. Figure 4 depicted the voltammetry curves of CO stripping for Pt-Ru. An anodic peak potential at approximate 0.55 V was observed in the stripping curves of Pt-Ru when CO was oxidized to  $\text{CO}_2$ . It was obvious that no CO oxidation peak existed following stripping, confirming that CO was thoroughly removed after the stripping scan process of CO. This indicated that the catalytic active sites were hindered. The CO stripping charge, which determined the ECSA corresponding, was determined through the calculation of the difference of the the voltammogram areas between the following two sweeps. Assuming only a monolayer

adsorption of CO on the surface of the catalyst, the ESCA of the Pt-Ru was calculated with a charge density of 0.39 mC/cm and also normalized based on the Pt loading, where an ECSA of around 77 m<sup>2</sup>/g was obtained for the Pt-Ru catalyst.

The charge transfer resistance ( $R_{ct}$ ), which was in relation with the electrochemical reaction, also determined the electro-catalytic capacity of Pt-Ru except for ECSA. Thus, electrochemical impedance spectroscopy (EIS) was employed to investigate the charge transfer resistance of Pt-Ru towards the electro-oxidation of methanol.

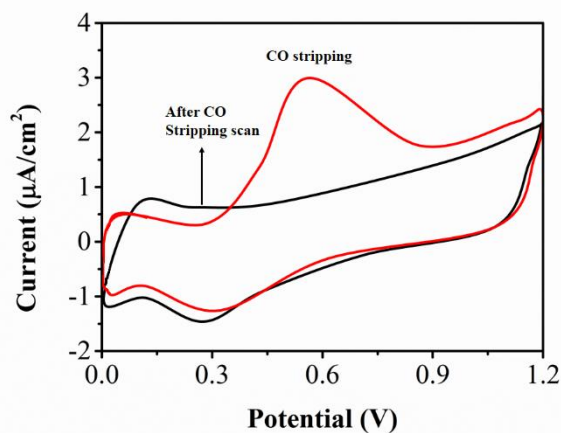


**Figure 4.** The CO stripping voltammetry curves of Pt-Ru. Conditions: electrolyte: 0.5 M H<sub>2</sub>SO<sub>4</sub>. Temperature: 25 °C.

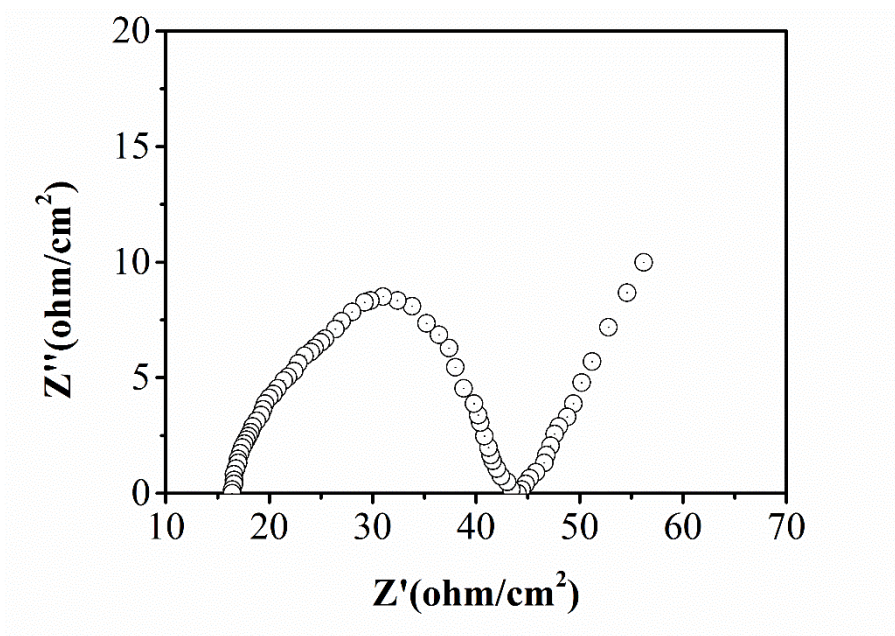


**Figure 5.** EIS spectra of the Pt-Ru. Condition: potential: 0.65 V; electrolyte: 0.5 M H<sub>2</sub>SO<sub>4</sub> + 0.5 M and methanol; temperature: 40 °C.

Besides, the ohmic resistance ( $R_{\square}$ ) of the electro-catalytic materials, which was further utilized for the  $iR_{\square}$ -correction of LSV curves discussed later in detail, was also determined by EIS. Figure 5 clarified the EIS plots of Pt-Ru, which were measured in the mixture of CH<sub>3</sub>OH (1M) and H<sub>2</sub>SO<sub>4</sub> (0.5

M) at around 0.65 V with a frequency ranging from 100 mHz to 100 KHz and an amplitude of 10 mV. The ZView software from Scribner Associates was used to model the impedance data with the  $R_s(R_eQ_1)(R_{ct}Q_{dl})$  circuit model to determine  $R_s$ ,  $R_e$  and  $R_{ct}$ . Here, the constant phase element was represented by  $Q_1$ , where the contribution donated by pseudocapacitance and double layer capacitance was represented with  $Q_{dl}$ .  $R_{ct}$  was determined by the diameter of the semi-circle at low frequency, which was lower than Pt-Ru ( $\sim 16.8 \Omega \text{ cm}^2$ ).

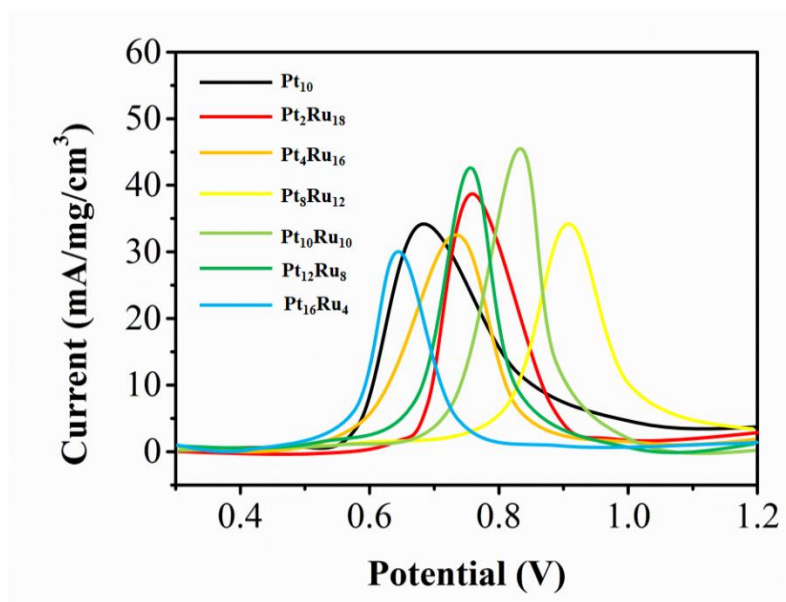


**Figure 6.** CV curves recorded in methanol with a concentration of 1 M. Condition: electrolyte: 0.5 M  $\text{H}_2\text{SO}_4$ ; Scan rate: 50 mV/s.

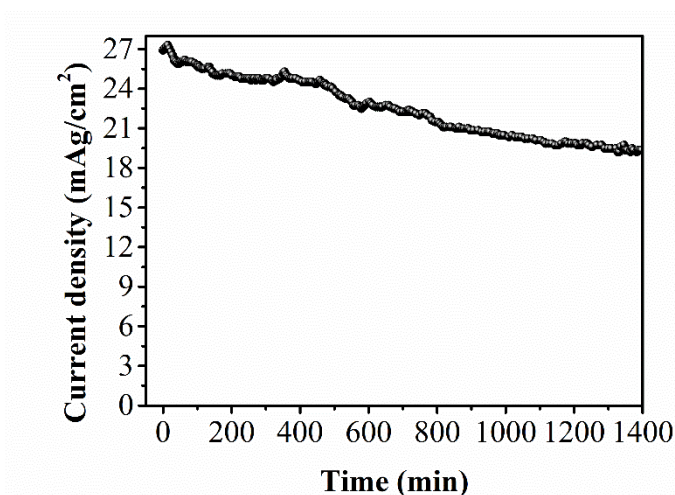


**Figure 7.** CA curves for Pt-Ru in methanol with a concentration of 1 M in the presence of  $\text{H}_2\text{SO}_4$  with a concentration of 0.5 M (750 mV) under atmospheric pressure at room temperature.

CVs was employed to measure the catalytic performances of the electrocatalysts based on Pt-Ru for the oxidation of methanol in a forward sweep. The current densities as well as peak potentials of the oxidation of methanol were illustrated in Figure 6, which varied when the composition of the

catalysts changed. The peak potential of methanol oxidation shifted to the negative direction with an increase in Pt content in the Pt–Ru electrocatalyst and displayed its lowest value with Pt<sub>10</sub>Ru<sub>10</sub>. The peak current density showed an opposite trend compared to the peak potential. The peak current density with Pt<sub>10</sub>Ru<sub>10</sub> had a higher value compared to that of the other catalysts [30, 31]. However, a converse trend was obtained with peak current density, where the peak current density of Pt<sub>10</sub>Ru<sub>10</sub> displayed a maximum value in comparison with that of other catalysts. In fact, the alloy of Pt and Ru with a molar ratio of 1:1 exhibits a high catalytic activity for oxidizing methanol. In this work, the surface ratio of Pt to Ru in the electrocatalyst deposited with Pt<sub>10</sub>Ru<sub>10</sub> electrolyte was approximate to 1:1.

In Figure 7, chronoamperometry (CA) was employed to assess the durability of the Pt–Ru catalyst with a potential of 750 mV for 1500 min. During this process, the specific current density of Pt mass for the catalyst reduced slightly. Based on the durability test, Pt<sub>10</sub>Ru<sub>10</sub>-based catalyst exhibited a stable catalytic activity for oxidizing methanol and strong tolerance against the poisoning of carbon monoxide. This performance is better than the reported other graphene–Pt systems, in which the current density decays at a much faster rate within 15–20 cycles due to the formation and gradual accumulation of intermediates such as CO<sub>ads</sub>, CH<sub>3</sub>OH<sub>ads</sub>, and CHO<sub>ads</sub> on the catalyst surface during the methanol oxidation reaction, significantly poisoning the Pt NPs for methanol oxidation [32, 33]

#### 4. CONCLUSIONS

An electrodeposition approach was employed to generate the electrocatalyst composed of Pt–Ru on the carbon paper, where the deposition parameters were tuned to control the catalyst particles density and size. Besides, the bulk as well as the molar ratios of the catalyst were determined by the component of the electrolytes. According to the XRD patterns, the catalyst exhibited an alloy structures. In particular, all the Pt–Ru electrocatalysts exhibited the catalytic activity towards the oxidation of methanol. Besides, the electrocatalysts also displayed the tolerance against the poisoning of carbon monoxide. A superior capacity was observed with the Pt<sub>10</sub>Ru<sub>10</sub>-based catalyst compared with the other catalysts. Besides, the Pt<sub>10</sub>Ru<sub>10</sub>-based catalyst also displayed a high electrochemical active surface area (ECSA) of 77 m<sup>2</sup>/g as well as a low resistance of charge transfer of 16.8 Ωcm<sup>2</sup>.

#### References

1. Z. Wang, J. Chen and L. Lin, *Energy & Environmental Science*, 8 (2015) 2250.
2. G. Zhu, B. Peng, J. Chen, Q. Jing and Z. Wang, *Nano Energy*, 14 (2015) 126.
3. S. Chatrchyan, V. Khachatryan, A. Sirunyan, A. Tumasyan, W. Adam, T. Bergauer, M. Dragicevic, J. Erö, C. Fabjan and M. Friedl, *Journal of High Energy Physics*, 2015 (2015) 1.
4. N. Kakati, S. Lee, J. Maiti and Y. Yoon, *Surface Science*, 606 (2012) 1633.
5. R. Cid, P. Fernández, J. Flores, S. Rojas, S. Rodríguez, E. Fatás and P. Ocón, *International Journal of Hydrogen Energy*, 37 (2012) 7119.
6. S. Kang, S. Lim, D.-H. Peck, S. Kim, D. Jung, S. Hong, H. Jung and Y. Shul, *International Journal of Hydrogen Energy*, 37 (2012) 4685.

7. R. Basnayake, Z. Li, S. Katar, W. Zhou, H. Rivera, E. Smotkin, D. Casadonte and C. Korzeniewski, *Langmuir*, 22 (2006) 10446.
8. S. Ahn, I. Choi, O. Kwon and J. Kim, *Chem. Eng. J.*, 181 (2012) 276.
9. B. Li, D. Higgins, S. Zhu, H. Li, H. Wang, J. Ma and Z. Chen, *Catalysis Communications*, 18 (2012) 51.
10. Z. Wei, L. Li, Y. Luo, C. Yan, C. Sun, G. Yin and P. Shen, *J Phys Chem B*, 110 (2006) 26055.
11. R. Jana, B. Maity, S. Mallick, A. Majumdar and P. Singh, *Indian Chemical Engineer*, 57 (2015) 103.
12. P. Prapainainar, A. Theampetch, P. Kongkachuichay, N. Laosiripojana, S. Holmes and C. Prapainainar, *Surface and Coatings Technology*, 271 (2015) 63.
13. W. Lee, S.C. Gil, H. Kim, K. Han and H. Lee, *Composites Science and Technology*, 129 (2016) 101.
14. Z. Wang, P. Zuo, G. Wang, C. Du and G. Yin, *J Phys Chem C*, 112 (2008) 6582.
15. A. Calabriso, L. Cedola, L. Del Zotto, F. Rispoli and S. Santori, *Journal of Cleaner Production*, 88 (2015) 23.
16. D. Yang, K. Sim, H. Kwen and S. Choi, *Journal of Industrial and Engineering Chemistry*, 18 (2012) 538.
17. L. Xiong and A. Manthiram, *Journal of the Electrochemical Society*, 152 (2005) A697.
18. Z. Cui, C. Liu, J. Liao and W. Xing, *Electrochimica Acta*, 53 (2008) 7807.
19. S. Rojas, F. García, S. Järas, M. Huerta, J. Fierro and M. Boutonnet, *Applied Catalysis A: General*, 285 (2005) 24.
20. T. Schmidt, H. Gasteiger and R. Behm, *Electrochemistry Communications*, 1 (1999) 1.
21. J. Jow, S. Yang, H. Chen, M. Wu, T. Ling and T. Wei, *International Journal of Hydrogen Energy*, 34 (2009) 665.
22. A. Caillard, C. Coutanceau, P. Brault, J. Mathias and J. Léger, *Journal of Power Sources*, 162 (2006) 66.
23. S. Woo, I. Kim, J.K. Lee, S. Bong, J. Lee and H. Kim, *Electrochimica Acta*, 56 (2011) 3036.
24. Z. He, J. Chen, D. Liu, H. Zhou and Y. Kuang, *Diamond and Related Materials*, 13 (2004) 1764.
25. F. Nieto, T. Catacora and C. Cabrera, *Journal of Electroanalytical Chemistry*, 571 (2004) 15.
26. X. Lu, J. Hu, J. Foord and Q. Wang, *Journal of electroanalytical chemistry*, 654 (2011) 38.
27. D. Chu and S. Gilman, *Journal of The Electrochemical Society*, 143 (1996) 1685.
28. M. Tsai, T. Yeh and C. Tsai, *Electrochemistry communications*, 8 (2006) 1445.
29. E. Pastor and V. Schmidt, *Journal of Electroanalytical Chemistry*, 383 (1995) 175.
30. L. Chan, R. Allen and K. Scott, *Journal of Power Sources*, 161 (2006) 11.
31. C. Roth, N. Benker, M. Mazurek, F. Scheiba and H. Fuess, *Applied Catalysis A General*, 319 (2007) 81.
32. J. Qiu, G. Wang, R. Liang, X. Xia and H. Yu, *J Phys Chem C*, 115 (2011) 15639.
33. N. Shang, P. Papakonstantinou, P. Wang and S.R.P. Silva, *J Phys Chem C*, 114 (2010) 15837.